

Pilot Symbol Assisted High Speed Packet Transmission System based on Adaptive OFDM in Broadband Mobile Channel

Chang-Jun Ahn and Iwao Sasase

Abstract: 4G mobile communication system requires the throughput of 10-100Mbps. Adaptive modulated OFDM system is promising technique for increasing the throughput. In the pilot symbol assisted high-speed packet transmission system, the data symbol duration is generally considered to be small compared to the coherence time. However, OFDM symbol duration is longer than the symbol duration of a single carrier system, so that the packet duration of the pilot symbol assisted high speed packet transmission system is long. In this case, the change of channel conditions is too fast to be accurately estimated by channel estimator at the receiver in high Doppler frequency, so that many errors occur during demodulation, especially with the data symbols at the end of each packet. In this paper, we consider the BER at various instantaneous E_b/N_0 that includes the demodulation errors in high Doppler frequency. When the coherence time is ten times longer than the duration of a single packet, the channel can be closely approximated as an AWGN channel. Otherwise, the approximation breaks down and the above-mentioned errors that occur during demodulation must be taken into consideration. In this paper, we propose the pilot symbol assisted high speed packet transmission system based on adaptive OFDM using a novel lookup table to consider the demodulated errors and evaluate the throughput performance.

Index Terms: High-speed packet transmission, adaptive OFDM, instantaneous E_b/N_0 , coherence time.

I. INTRODUCTION

Mobile radio communication systems are increasingly demanded to provide a variety of high-quality multimedia services to mobile users. To meet this demand, modern mobile radio transceiver systems must be able to support high capacity, variable bit rate information transmission and high bandwidth efficiency. In the mobile radio environment, signals are usually impaired by fading and multi-path delay phenomenon. In such channels, severe fading of the signal amplitude and intersymbol-interference (ISI) due to the frequency selectivity of the channel cause an unacceptable degradation of the error performance.

Manuscript received July 19, 2002.

This paper was originally submitted to the special issue on 3G/4G, December 2002.

C.-J. Ahn is with the Communication Research Laboratory (CRL), Independent Administrative Institution, Yokosuka, 239-0837, Japan, e-mail: jun@sasase.ics.keio.ac.jp.

I. Sasase is with the Department of Information and Computer Science, Keio University, Yokohama, 223-8522, Japan, e-mail: sasase@ics.keio.ac.jp.

OFDM is an efficient scheme to mitigate the effect of multi-path channel, since it eliminates ISI by inserting guard interval longer than the delay spread of the channel [1], [2]. Therefore, OFDM is generally known as an effective technique for high data rate services such as digital audio broadcasting (DAB) and digital video broadcasting (DVB). Recently, OFDM has been considered as one of the promising modulation candidates for a fourth generation broadband mobile communication system for this reason.

Most OFDM systems use a fixed modulation scheme over all carriers for simplicity. However, each carrier in an OFDM system can potentially have a different modulation scheme depending on the channel conditions. Any coherent or differential, phase or amplitude modulation scheme including BPSK, QPSK, 8PSK, and 16QAM can be used. Each modulation scheme provides a trade off between spectral efficiency and the bit error rate (BER). Choosing the highest M-ary modulation scheme that will give an acceptable BER can maximize the spectral efficiency. Thus, adaptive modulation scheme is the efficient scheme to increase the throughput performance.

Steele [3]–Sampei [6] propose and simulate burst by burst adaptive QAM for exploiting the time-variant Shannonian channel capacity of narrowband fading channel, and variable concatenated coded scheme, respectively. Yoshiki proposes adaptive QAM with power control [7]. Chi-Hsiao, Desai, and Rohling evaluate OFDM based wireless networks using adaptive modulation [8]–[10]. It is assumed in an adaptive modulation scheme that the transmitter has full knowledge of the channel state information (CSI), and that the channel is slowly-varying. Above mentioned studies demonstrating the performance gain of adaptive modulation have assumed the availability of the packet duration that is enough smaller than the coherence times, and perfect channel estimation.

In the pilot symbol assisted high-speed packet transmission (PSAPT) system [11], [12], the data symbol duration is generally considered to be small compared to the coherence time. During the packet duration less than the coherence time, the channel can be well approximated as an AWGN channel. So we can use the Shannonian channel capacity theory to set the threshold E_b/N_0 for adaptive modulation. However, OFDM symbol duration is longer than the symbol duration of a single carrier, therefore, the packet duration of PSAPT system based on adaptive OFDM is increased. In this case, the change of channel conditions is too fast to be accurately estimated by channel estimator at the receiver in high Doppler frequency, so that many errors occur in data demodulation processing particularly in the

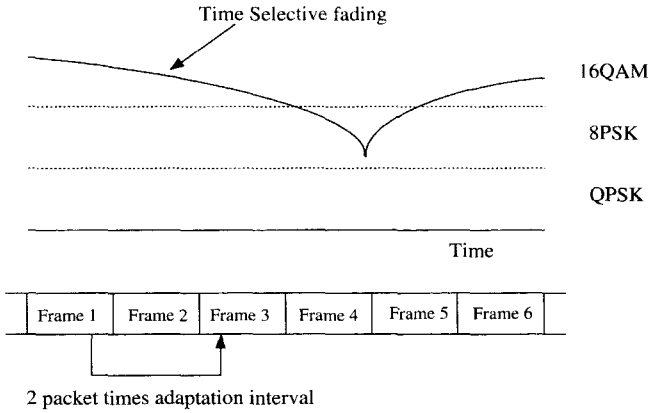


Fig. 1. The concept of adaptive all carrier modulation (AAM) for time selective channel.

last part of the packet.

In this paper, we consider the BER at various instantaneous E_b/N_0 that includes the demodulation errors in high Doppler frequency. When the coherence time is ten times longer than the duration of a single packet, the channel can be closely approximated as an AWGN channel. Otherwise, the above-mentioned errors that occur during demodulation must be taken into consideration. We propose a novel lookup table take into account the demodulated errors in high Doppler frequency and evaluate the system performance.

This paper is organized as follows. Conventional adaptive modulation system is described in Section II. In Section III, we describe our proposed adaptive modulation scheme. In Section IV, we describe the simulation conditions and show the simulation results. Finally, the conclusion is given in Section V.

II. ADAPTIVE MODULATION FOR OFDM

A. Conventional Adaptive Modulation Scheme

The general concept of an adaptive modulation for time variant channel is shown in Fig. 1. The adaptive modulation needs to get the propagation path conditions, which vary over time. The system uses a feedback information in which the system can know the conditions in a reception frame and can choose one of the modulation schemes in the transmitter. When the transmission conditions such as signal strength change, the modulation scheme for the transmission may be changed for adaptation interval. In this case, all subcarriers use the same modulation scheme, that is called adaptive all carrier modulation (AAM).

Since the propagation characteristic of the each subcarriers differ in frequency selective fading channels, adaptive subcarrier modulation (ASM) scheme may obtain good throughput by selecting a suitable modulation scheme for each subcarrier adaptively. The concept of an adaptive modulation system for OFDM with ASM is shown in Fig. 2 for the time and frequency domain expressions, respectively.

B. Conventional Decision Threshold for Adaptive Modulation

In the conventional adaptive modulation system, the packet duration is considered to be small enough compared to the co-

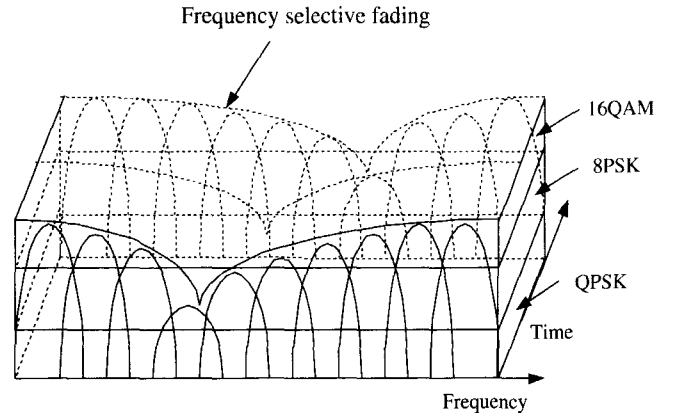


Fig. 2. The concept of adaptive subcarrier modulation (ASM) for frequency and time selective channel.

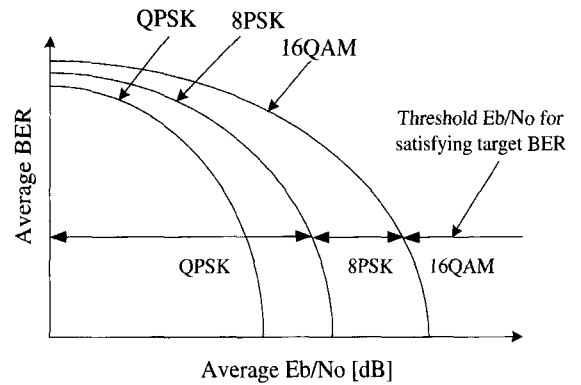


Fig. 3. BER curve of various modulation schemes to set the lookup Table 1 under the AWGN channel.

herence time. During a packet duration less than the coherence time, the channel can be well approximated by an AWGN channel. So we can read the lookup table like the Fig. 3 to satisfy the target BER.

Moreover, for a given symbol error probability of OFDM, we can calculate the required SNR for each of the different modulation schemes used. The thresholds for changing from one modulation scheme to another are obtained by using the required SNR. Symbol error probability due to Gaussian noise for MPSK is given by [13]

$$P_M \leq 1 - \left[1 - 2Q\left(\sqrt{\frac{3E_s}{(M-1)N_0}}\right) \right]^2, \quad (1)$$

where the average symbol energy, E_s , the noise power, N_0 , and the modulation scheme, M , respectively. The Gaussian cumulative distribution function, $Q(x)$ is expressed as

$$Q(x) = \frac{1 - \text{erf}\left(\frac{x}{\sqrt{2}}\right)}{2}, \quad (2)$$

where the error function $\text{erf}(x)$ is

$$\text{erf}(x) = \frac{2}{\sqrt{\pi}} \int_0^x e^{-t^2} dt. \quad (3)$$

By solving (1) for $\frac{E_s}{N_0}$ and using (2) and (3), we obtain the

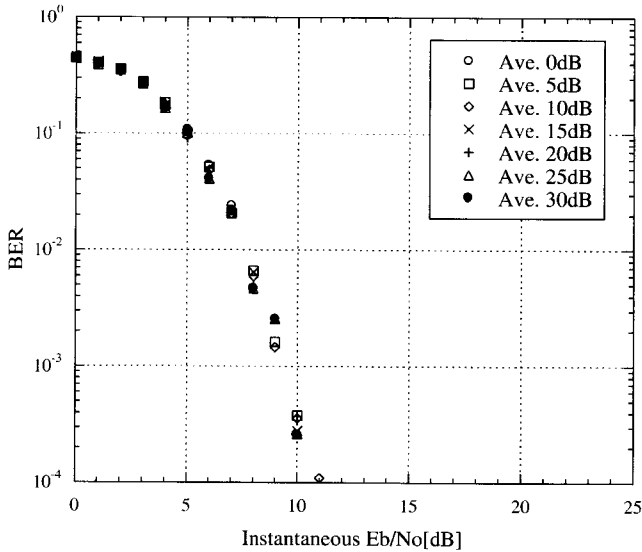


Fig. 4. BER performance of instantaneous E_b/N_0 for various average E_b/N_0 of 8PSK, $F_d=10\text{Hz}$.

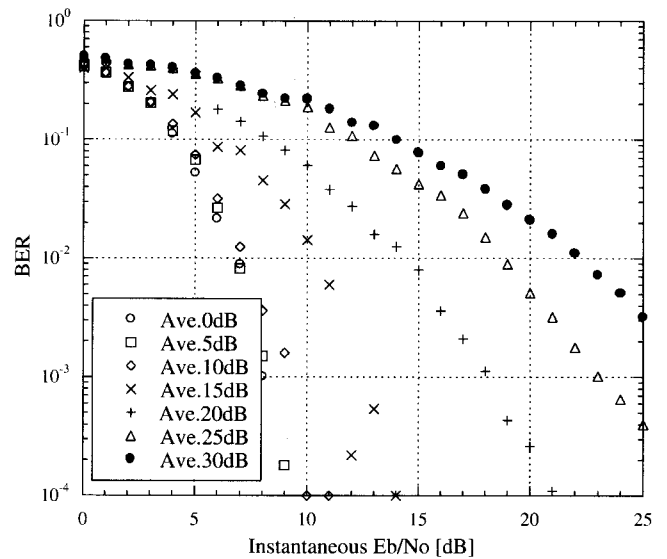


Fig. 5. BER performance of instantaneous E_b/N_0 for various average E_b/N_0 of 8PSK, $F_d=80\text{Hz}$.

Table 1. Threshold E_b/N_0 of lookup Table 1 and 2 for satisfying the target BER of 10^{-3} [dB].

Mod.	lookup Table 1	lookup Table 2
QPSK	$-\infty$	$-\infty$
8PSK	21	27 / 42.5 (10 / 80 Hz)
16QAM	21.7	34 / 53.5 (10 / 80 Hz)

E_s/N_0 required for a given M , and certain symbol error probability, P_M

$$\frac{E_s}{N_0} \geq \frac{2(M-1)}{3} \left[\text{erf}^{-1}(\sqrt{1-P_M}) \right]^2. \quad (4)$$

Table 1 shows the threshold E_b/N_0 of the conventional adaptive modulation schemes based on the AWGN channel (lookup Table 1) and average E_b/N_0 has been read from the BER of flat fading (lookup Table 2) for satisfying the target BER of 10^{-3} at $F_d = 10, 80\text{Hz}$.

III. PROPOSED SYSTEM

Suppose a packet consists of $100 \sim 512$ subcarriers and 64 OFDM symbols (number of pilot symbols is $N_p=4$ and number of data symbols is $N_d=60$), and transmission rate is considered about $100 \sim 150$ Ksymbols/s for individual subcarriers [11], [12]. If we assume that the mobile is travelling at approximately 4.8m/s (17km/h) and operating at 5 GHz, the Doppler frequency is approximately $F_d=80\text{Hz}$. The Jakes correlation between two fading coefficients t time samples apart is $J_0(2\pi F_d T_s t)$, where T_s is the symbol period and J_0 is the zeroth order Bessel function of the first kind. We assume that $T_s=1/122500=8.16\mu\text{s}$, so $T_s F_d=0.000653$.

In wireless communication system, the coherence time of

Doppler frequency of 80Hz can be represented by [14]

$$\begin{aligned} T_c &\simeq \frac{9}{16\pi F_d} = \frac{9 \cdot C}{16\pi \cdot v \cdot f_o} \\ &= \frac{9 \times 3 \times 10^8}{16 \times 3.14 \times 4.8 \times 5 \times 10^9} = 2239\mu\text{s}. \end{aligned} \quad (5)$$

where F_d is the maximum Doppler frequency given by $F_d = v \cdot f_o/C$, f_o is the operating frequency, v is the mobile speed and C is the light speed. From (5), fading samples separated by much less than 274 symbols, say $T_c = 274$ symbols, are approximately equal for $F_d = 80\text{Hz}$. It means that the coherence time is equal to the duration of only 4.29 packets.

By the way, the previous adaptive modulation studies demonstrating the performance gain of adaptive modulation have assumed the availability of the packet duration that is enough smaller than the coherence times such as wireless ATM packet structure, and perfect channel estimation. The wireless ATM packet is considered with 12 OFDM symbols (number of pilot symbols is $N_p=2$ and number of data symbols is $N_d=10$), and operating at 2GHz. In this case, the coherence time is $T_c=551$ symbols, so that the coherence time of the wireless ATM is about 46 packet times. Therefore, the wireless ATM can compensate the effect of fading. However, the PSAPT system shows error floor in high Doppler frequency because the packet duration is not enough smaller than the coherence time.

Fig. 4 and Fig. 5 show the BER at various instantaneous E_b/N_0 due to the Doppler frequency of 10 and 80Hz with 8PSK. The instantaneous E_b/N_0 is defined as the ratio between the signal power that is effected by the Doppler frequency and background noise for individual subcarrier, and the average E_b/N_0 is defined as the average ratio between the signal power and noise for whole subcarriers. When the transmitted signal is deep faded by the Doppler frequency, the faded signal's power is decreased. Therefore, the instantaneous E_b/N_0 is degraded. Fig. 4 shows the same BER at various instantaneous E_b/N_0 due to the Doppler frequency for various average E_b/N_0 at Doppler

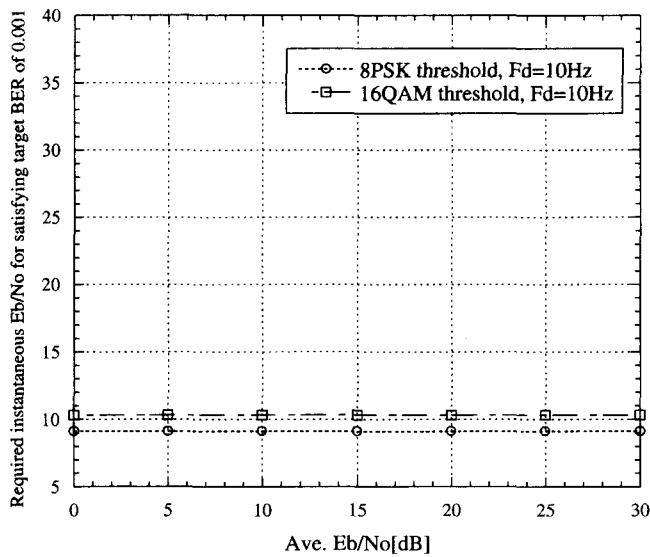


Fig. 6. Required instantaneous E_b/N_0 for satisfying the target BER of 10^{-3} , $F_d=10\text{Hz}$.

frequency of 10 Hz with 8PSK. Since the channel is slowly changed at Doppler frequency of 10Hz, Doppler frequency is perfectly compensated by using the pilot symbol's channel state information. Therefore, the demodulation property depends on an AWGN channel characteristic. In Doppler frequency of 10Hz, the coherence time is about $T_c = 17905\mu s$, so that it is about 34 packet times. This coherence time is long enough for the perfect channel compensation. The coherence time, however, decreases with increasing Doppler frequency. As a result, the system cannot compensate for the Doppler frequency, and many errors are made in demodulating the data symbols near the end of each packet. Thus, the BER vs. instantaneous E_b/N_0 curves (as a function of average E_b/N_0) are different when the Doppler frequency is taken into consideration.

For example, Fig. 5 shows that high average E_b/N_0 like 20dB causes worse BER performance than those of 0, 5 and 10dB. This is because the instantaneous E_b/N_0 includes the effect of the Doppler frequency compensation errors. When the Doppler frequency is high, however, the coherence time becomes shorter and the channel is no longer perfectly compensated. Particularly, when the instantaneous E_b/N_0 is smaller than the average E_b/N_0 , the received signals are strongly effected by the background noise. For the instantaneous E_b/N_0 of 10dB, the powers are decreased from average E_b/N_0 of 0, 5, 10, and 20dB about 10dB, 5dB, 0dB, and -10dB by the Doppler frequency, respectively. Particularly, the power of the instantaneous E_b/N_0 of 10dB from the average E_b/N_0 of 20dB is largely decreased. In this case, the power of the instantaneous E_b/N_0 of 10dB from the average E_b/N_0 of 20dB has been strongly affected by the background noise, and the demodulation is not more accurate than those of small shifted signals. It means that large decreased signal causes worse BER than those of small decreased signals in high Doppler frequency.

The power of the instantaneous E_b/N_0 of 10dB from the average E_b/N_0 of 0dB is also shifted. However, in this case, the signal power is increased by the Doppler frequency. So the power

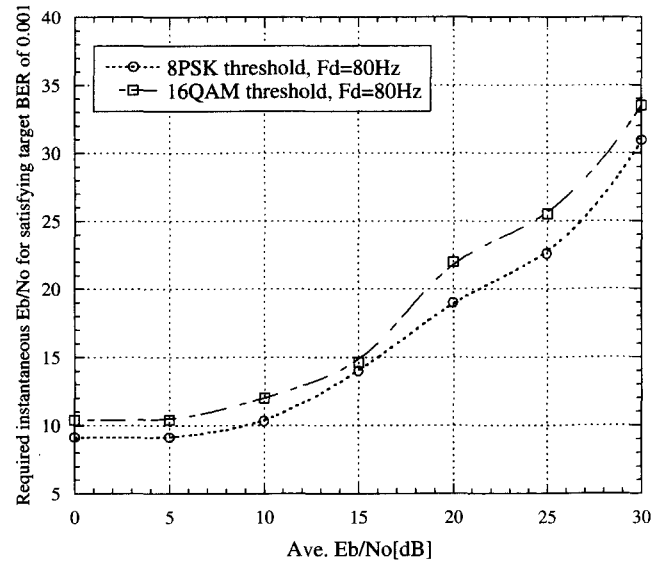


Fig. 7. Required instantaneous E_b/N_0 for satisfying the target BER of 10^{-3} , $F_d=80\text{Hz}$.

Table 2. Required instantaneous E_b/N_0 as a lookup table for target BER of 10^{-3} at $F_d = 10, 80\text{Hz}$ [dB].

Average E_b/N_0	Modulation	10Hz	80Hz
0	8PSK	8.4	8.4
	16QAM	10.4	10.4
5	8PSK	8.4	8.4
	16QAM	10.4	10.6
10	8PSK	8.4	10.3
	16QAM	10.4	12
15	8PSK	8.4	14
	16QAM	10.4	14.2
20	8PSK	8.4	19
	16QAM	10.4	22
25	8PSK	8.4	22.6
	16QAM	10.4	25.5
30	8PSK	8.4	30.9
	16QAM	10.4	33.5

from the average E_b/N_0 of 0dB has been weakly affected by the background noise. Thus the demodulation is more accurate than that of the power of the instantaneous E_b/N_0 of 10dB from the average E_b/N_0 of 20dB. When we use the conventional adaptive modulation lookup table as lookup Table 1 for PSAPT system, the throughput is degraded. On the other hand, when we change the modulation scheme for individual subcarrier with considering above simulated results as Fig. 6 and Fig. 7, we can reduce the throughput degradation in high Doppler frequency.

Fig. 6 and Fig. 7 show the required instantaneous E_b/N_0 for high speed packet transmission system. The required instantaneous E_b/N_0 depends on the modulation scheme that is used for the subcarrier, and determines the system's target BER. Fig. 6 and Fig. 7 give an overview of these levels, which have been read from the BER curves for the different modulation schemes for satisfying the target BER of 10^{-3} at $F_d = 10, 80\text{Hz}$ using these figures. By using these figures, we can make a lookup Table 3 as Table 2. Table 2 shows the required instantaneous E_b/N_0 of our proposed adaptive scheme (lookup Table 3) for

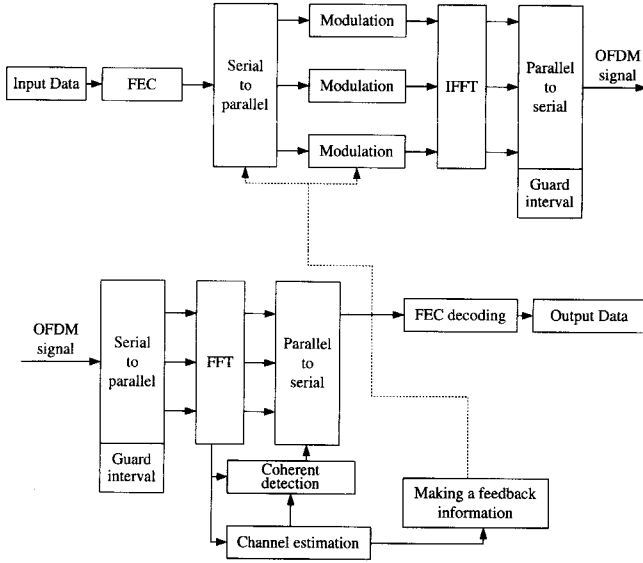


Fig. 8. Simulation model.

Table 3. Simulation parameters.

Modulation	QPSK, 8PSK, 16QAM
Demodulation	Coherent detection
Data rate	15.68 Msymbol/s
FFT size	128
Number of carriers	128
Guard interval	25 sample times
Frame size	64 symbols ($N_p = 4, N_d = 60$)
FEC	convolutional code ($R=1/2, K=7$)
Fading	18 path Rayleigh fading
Doppler frequency	10, 80 Hz
Adaptation interval	2 packet times

target BER of 10^{-3} based on the modulation scheme that is used for the subcarrier.

IV. COMPUTER SIMULATED RESULTS

A. System Description

Fig. 8 shows the simulation model for adaptive modulation based on OFDM with $N_c = 128$ subcarriers. In the transmitter side, data stream is first encoded. Here, convolutional codes (rate $R = 1/2$, constraint length $K = 7$) are used, which have turned out to be efficient for transmission of an OFDM signal over frequency selective fading channel [15], [16]. The coded bits are then mapped to the modulation symbols of $N_c = 128$ subcarriers. The OFDM time signal is generated by an inverse FFT and is transmitted over the frequency selective and time variant radio channel after the cyclic extension has been inserted. The transmitted signals are subject to broadband channel propagation as shown in Fig. 9 [17], [18]. In this model, $L = 18$ path Rayleigh fadings have exponential shapes with path separation $T_{path} = 42nsec$. This case causes a severe frequency selective fading. The maximum Doppler frequency is assumed to be 10Hz and 80Hz. In the receiver side, the received

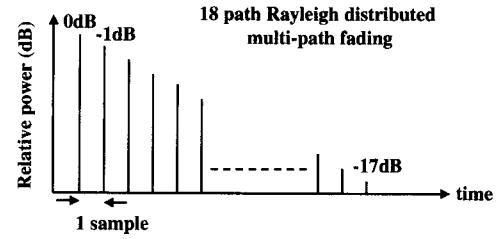


Fig. 9. Channel model.

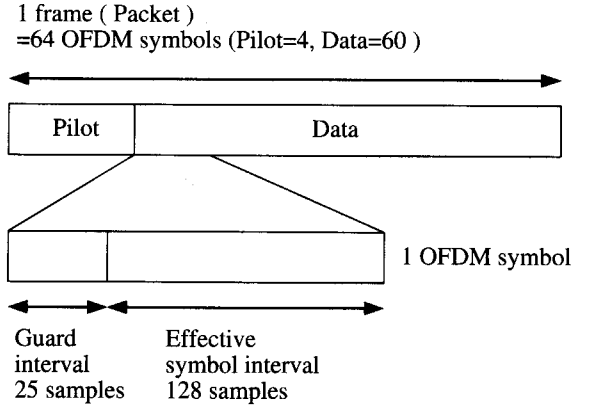


Fig. 10. Packet structure.

signals are serial to parallel converted and N_c parallel sequences are passed to a FFT operator, which converts the signal back to the frequency domain. This frequency domain signals are coherently demodulated by using a pilot signal. After demodulation, the binary data is decoded by the Viterbi soft decoding algorithm. The simulation parameters are listed in Table 3. Fig. 10 shows packet structure. Packet consists of 128 subcarriers and 64 OFDM symbols (number of pilot signals: $N_p = 4$, number of data: $N_d = 60$).

B. Simulation Results

In the following simulation results, throughput η (bit per second) is defined as

$$\eta = R_b \times \frac{N_{suc}}{N_{trans}}, \quad (6)$$

where R_b is the total information bit rate, and N_{trans} and N_{suc} are the total number of transmitted and correctly received packets, respectively. Here, we evaluate the performance of adaptive modulation using an adaptation interval of 2 packet durations, which should accommodate the delay and processing time of the feedback information (FBI) from the receiver to the transmitter. FBI includes the estimated channel state information like power and noise level of individual subcarriers. In the adaptive modulation systems, above mentioned FBI is required. But FBI is generally assumed to be infinitely precise and perfect. In the practical case, it is necessary to have some delay times to transmit the FBI from receiver to transmitter. Moreover, the system requires the processing time to make an adaptive modulation command using the FBI at the transmitter. With the FBI delay and the processing time to make an adaptive modulation, the

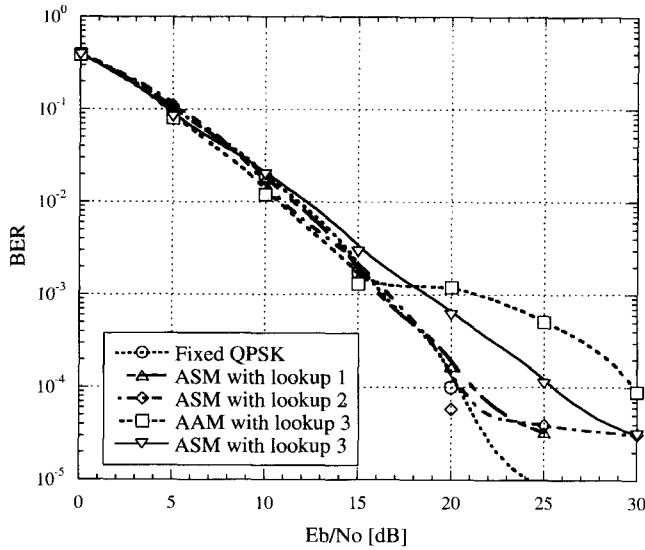


Fig. 11. BER of fixed QPSK, ASM with lookup Table 1, ASM with lookup Table 2, AAM with lookup Table 3, and ASM with lookup Table 3 for target BER of 10^{-3} , and $F_d = 10$ Hz.

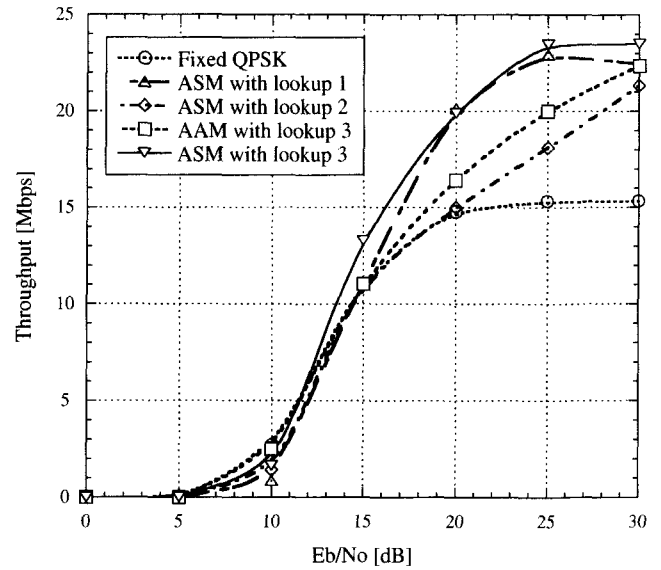


Fig. 12. Throughput of fixed QPSK, ASM with lookup Table 1, ASM with lookup Table 2, AAM with lookup Table 3, and ASM with lookup Table 3 for target BER of 10^{-3} , and $F_d = 10$ Hz.

system performance might be degraded. In this evaluation, LMS method is used to fit a second order polynomial to each of the measured channel impulse responses [19]. To maintain the system performance, we calculate the next fading for 2 packet times later using this polynomial values for increasing the accuracy of the FBI.

Fig. 11 and Fig. 12 show the BER and throughput of fixed QPSK, adaptive subcarrier modulation (ASM) with lookup Table 1, adaptive subcarrier modulation (ASM) with lookup Table 2, adaptive all carrier modulation (AAM) with lookup Table 3, adaptive subcarrier modulation (ASM) with lookup Table 3 for target BER of 10^{-3} , and $F_d = 10$ Hz. The system based on lookup Table 3 shows poor BER performance. Particularly, AAM with lookup Table 3 shows the error floor between 15dB and 20dB. But the throughput performance shows better than the lookup Table 1 and 2. This is because the lookup Table 3 is made from the instantaneous E_b/N_0 , so the system accurately selects the modulation schemes from the estimated channel state. However, in low Doppler frequency, the coherence time is enough larger than the packet duration. Therefore, the lookup Table 1 and lookup Table 3 show approximately same values. For this reason, the throughput of the system based on lookup Table 3 is not larger than that of the system based on lookup Table 1. Moreover, ASM may obtain better throughput than AAM by selecting a suitable modulation scheme for each subcarrier adaptively.

Fig. 13 and Fig. 14 show the BER and throughput of fixed QPSK, ASM with lookup Table 1, ASM with lookup Table 2, AAM with lookup Table 3, and ASM with lookup Table 3 for target BER of 10^{-3} , and $F_d = 80$ Hz. In Fig. 13 and Fig. 14, ASM scheme with lookup Table 1 shows poor BER than that of the fixed modulation, since the ASM scheme with lookup Table 1 uses the threshold E_b/N_0 based on the AWGN channel and this lookup table does not consider the demodulation errors. Moreover, with increasing the E_b/N_0 , the BER of ASM scheme with lookup Table 1 is degraded. This is because ASM

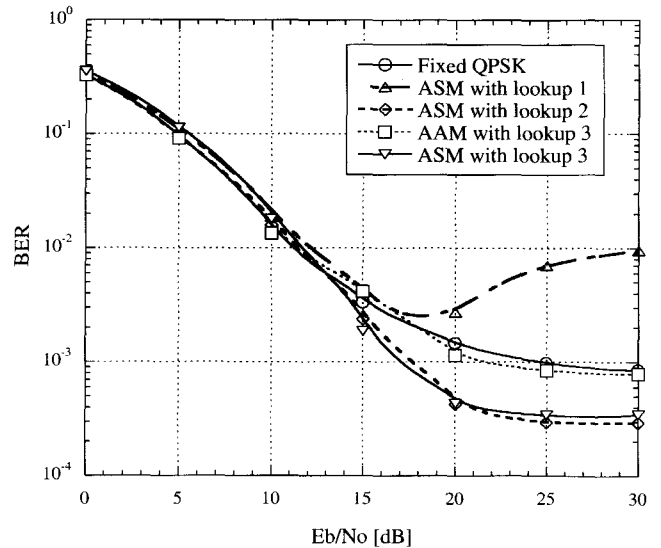


Fig. 13. BER of fixed QPSK, ASM with lookup Table 1, ASM with lookup Table 2, AAM with lookup Table 3, and ASM with lookup Table 3 for target BER of 10^{-3} , and $F_d = 80$ Hz.

scheme with lookup Table 1 generally changes channel modulation scheme based on the estimated channel state without considering Doppler frequency. In such a case, the lookup Table 1 based system has no meaning, even though the channel state is best. The lookup Table 2 based system achieves better BER than that of the lookup Table 1 based system and fixed QPSK. The lookup Table 3 is made from the instantaneous E_b/N_0 , so it more accurately selects the modulation scheme with considering the demodulation errors. Therefore, lookup Table 3 based system achieves the best throughput and satisfies the target BER.

Fig. 15 and Fig. 16 show the BER and throughput of AAM with lookup Table 3 with various feedback information (FBI) errors for target BER of 10^{-3} , and $F_d = 80$ Hz. When increasing the FBI errors, the BER is significantly degraded. This is

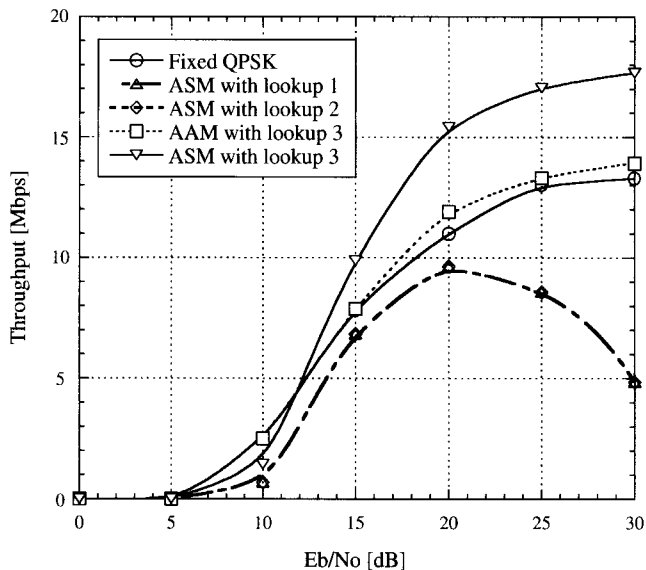


Fig. 14. Throughput of fixed QPSK, ASM with lookup Table 1, ASM with lookup Table 2, AAM with lookup Table 3, and ASM with lookup Table 3 for target BER of 10^{-3} , and $F_d = 80\text{Hz}$.

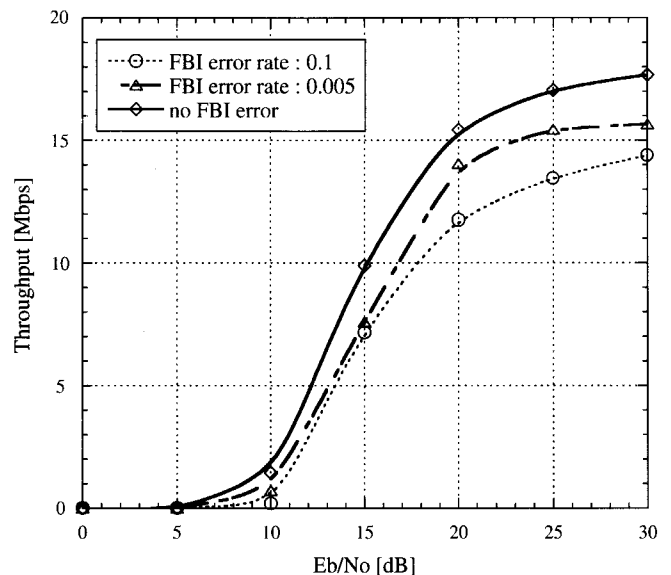


Fig. 16. Throughput of our proposed adaptive modulation scheme with FBI errors 10^{-1} , $5 \cdot 10^{-2}$, and no error for target BER of 10^{-3} , and $F_d = 80\text{Hz}$.

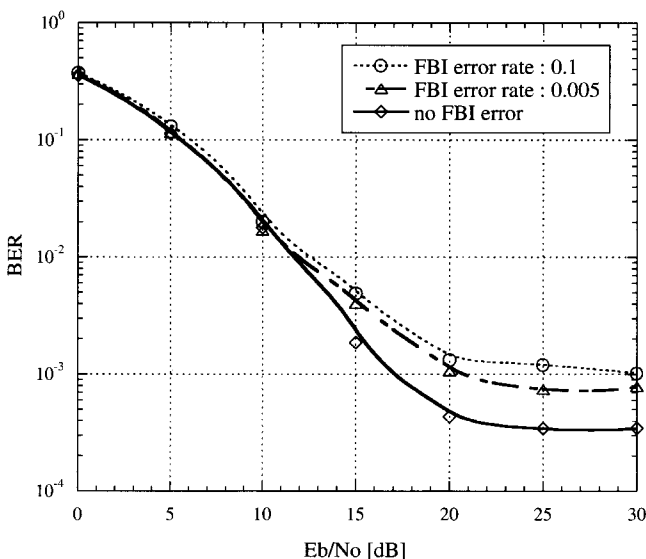


Fig. 15. BER of our proposed adaptive modulation scheme with FBI errors 10^{-1} , $5 \cdot 10^{-2}$, and no error for target BER of 10^{-3} , and $F_d = 80\text{Hz}$.

because the channel state and the selected modulation schemes using FBI with errors are different. The BER of the case with FBI errors of 10^{-1} occurs 7 times larger than that of the case with no FBI error. No FBI error case obtains the achievable maximum throughput about 17.8 Mbps at $E_b/N_0 = 30\text{dB}$, but the case with FBI errors of 10^{-1} obtains the achievable maximum throughput about 14.2Mbps at $E_b/N_0 = 30\text{dB}$.

V. CONCLUSION

In this paper, we have evaluated the pilot symbol assisted high speed packet transmission system based on adaptive OFDM in broadband mobile channel using various adaptive modulation schemes like AAM and ASM with lookup Table 1, 2, and 3. From the simulated results, ASM with lookup Table 3 satis-

fies the target BER and obtains better throughput than those of the fixed and conventional adaptive modulation schemes in high Doppler frequency.

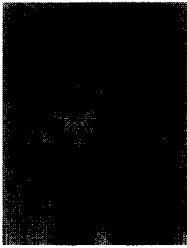
ACKNOWLEDGEMENTS

The authors would like to thank the anonymous reviewers for their comments and suggestions.

REFERENCES

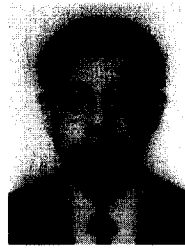
- [1] L. Cimini, "Analysis and simulation of a digital mobile channel using OFDM," *IEEE Trans. Commun.*, vol. 33, pp. 665–675, July 1985.
- [2] J. A. C. Bingham, "Multicarrier modulation for data transmission: An idea whose time has come," *IEEE Commun. Mag.*, vol. 28, pp. 5–14, May 1990.
- [3] R. Steele and W. Webb, "Variable rate QAM for data transmission over Rayleigh fading channel," in *Proc. wireless*, Calgary, Alberta, Canada, 1991, pp. 1–14.
- [4] T. Keller, T. H. Liew, and L. Hanzo, "Adaptive redundant residue number system coded multicarrier modulation," *IEEE J. Selected Areas Commun.*, vol. 18, no. 11, pp. 2292–2301, Nov. 2000.
- [5] L. Hanzo and W. Webb, *Single and Multicarrier Quadrature Amplitude Modulation*, Wiley-IEEE Press, 2000.
- [6] H. Masuoka *et al.*, "Adaptive modulation system with variable coding rate concatenated code for high quality multi-media communication systems," in *Proc. VTC'1996*, pp. 815–819, Piscataway, NJ, USA.
- [7] T. Yoshiki, S. Sampei, and N. Morinaga, "High bit rate transmission scheme with a multilevel transmit power control for the OFDM based adaptive modulation schemes," in *Proc. VTC 2001*, vol. 1, pp. 727–731, 2001.
- [8] Y. Chi-Hsiao and E. Geraniotis, "Adaptive modulation, power allocation and control for OFDM wireless networks," in *Proc. PIMRC 2000*, vol. 3, pp. 809–813, 2000.
- [9] K. Baum *et al.*, "Performance analysis of an adaptive OFDM packet data system," in *Proc. Int. Zurich seminar Broadband commun.*, pp. 237–243, 2000.
- [10] H. Rohling and R. Grunheid, "Adaptive coding and modulation in an OFDM-TDMA communication system," in *Proc. VTC 98*, vol. 2, pp. 773–776, 1998.
- [11] H. Atarashi, S. Abeta, and M. Sawahashi, "Performance evaluation of coherent high-speed Td-OFCDM broadband packet wireless access in forward link employing multi-level modulation and hybrid ARQ," *IEICE Trans. Fundamentals*, vol. E84-A, no. 7, pp. 1670–1680, July 2001.

- [12] S. Abeta *et al.*, "Performance of coherent multi-carrier/DS-SS and MC-SS for broadband packet wireless access," *IEICE Trans. Commun.*, vol. E84-B, no. 3, pp. 406–414, Mar., 2001.
- [13] Proakis, *Digital communications* McGraw-Hill 3rd ed., Singapore, 1995.
- [14] Available at <http://www.mprg.ee.vt.edu/publications/PHWComm/Tsr165.pdf>.
- [15] J. Cho *et al.*, "Optimal weighting for ML decoding of convolution code in COFDM systems," in *Proc. VTC 2001 Spring*, vol. 2, 2001, pp. 796–799.
- [16] L. Lang, L. Cimini, and J. C. Chuang, "Comparison of convolutional and turbo codes for OFDM with antenna diversity in high-bit-rate wireless applications," *IEEE Commun. Lett.*, vol. 4, no. 9, pp. 277–279, Sept. 2000.
- [17] M. Tano *et al.*, "Three-step cell search algorithm exploiting common pilot channel for OFCDM broadband wireless access," *IEICE Trans. Comm.*, vol. E86-B no. 1, pp.325-334, Jan. 2003.
- [18] N. Maeda, H. Atarashi, and M. Sawahashi, "Performance comparison of channel interleaving methods in frequency domain for VSF-OFCDM broadband wireless access in forward link," in *IEICE Trans. Commun.*, vol. E86-B no. 1 pp. 300–313, Jan. 2003.
- [19] H. Takahashi and M. Nakagawa, "Antenna and multicarrier combined diversity system," *IEICE Trans. Comm.*, vol. E79-B, no. 9, pp. 1221–1226, Sept. 1996.



Chang-Jun Ahn received the Ph.D. degree in the Department of Information and Computer Science in 2003 from Keio University, Japan. From 2001 to 2003, he was a research associate in the Department of Information and Computer Science, Keio University. Currently, he is working at the Communication Research Laboratory (CRL), Independent Administrative Institution, Japan, as a researcher. His current research interests include OFDM, digital communication, channel coding, and signal processing for telecommunications. He is a member of the IEE, the

IEICE, and the IEEE.



Iwao Sasase was born in Osaka, Japan, in 1956. He received the B.E., M.E., and Ph.D. degrees in Electrical Engineering from Keio University in 1979, 1981 and 1984, respectively. From 1984 to 1986, he was a Post Doctoral Fellow and Lecturer of Electrical Engineering at University of Ottawa, Canada. He is now a Professor of Information and Computer Science at Keio University, Japan. His research interest include modulation and coding, mobile communications, optical communications, communication networks, power electronics and information theory. He

published more than 185 journal papers and 276 international conference papers. He received the 1984 IEEE Communication Society Student Paper Award (Region 10), 1986 Inoue Memorial Young Engineer Award, 1988 Hiroshi Ando Memorial Young Engineer Award, and 1988 Shinohara Memorial Young Engineer Award, and 1996 IEICE Switching System Technical Group Best Paper Award. He is a senior member of the IEEE, a member of Information Processing Society of Japan, and the Society of Information Theory and Its Applications (SITA), Japan.